Relativistic wave-function effect on the *K*-shell ionization of Sb, Gd, Yb, Au, and Bi by low- to intermediate-velocity F ions

D. Mitra,[1] Yeshpal Singh,[1] Lokesh C. Tribedi,[1] P. N. Tandon,[1] and D. Trautmann[2]
[1]*Tata Institute of Fundamental Research, Homi Bhabha Road, Colaba, Mumbai 400 005, India*
[2]*Institute für Theoretische Physik, Universität Basel, Klingelbergstrasse 82, CH-4056 Basel, Switzerland*
(Received 11 August 2000; published 13 June 2001)

We have measured absolute cross sections for the *K*-shell ionization of medium- and high-*Z* targets of Sb, Gd, Yb, Au, and Bi induced by low- to intermediate-velocity F ions having energies between 2.5 and 5.8 MeV/u. Our main interest is to see the effect of the relativistic nature of the *K*-shell electrons of these target atoms on the ionization cross sections. The information on the degree of relativistic effect has been obtained by comparing the measured data with different theoretical calculations with and without including the relativistic corrections. A comparative study of the two different models such as SCA (semiclassical approximation) and ECPSSR [perturbed stationary state (PSS) including the corrections for energy (E) loss, Coulomb (C) deflection, and relativistic (R) effects] is presented. It is shown that the SCA calculations with the relativistic wave function predict an ionization cross section that is at least an order of magnitude higher compared to that given by the nonrelativistic calculation for Bi target. This factor is reduced to about 2 in the case of Sb. The ECPSSR, however, predicts lower ratios for the relativistic to nonrelativistic calculations. The experimental results, in general, are in good agreement with the SCA calculations using relativistic wave functions as well as with the ECPSSR model. For high-*Z* targets the SCA gives slightly better agreement with the data compared to the ECPSSR. In addition, it is shown that in the ECPSSR formalism the ionization cross sections of high-*Z* (with large relativistic effect) as well as low-*Z* targets (with less relativistic effect) can be scaled approximately to follow a universal curve after including the relativistic correction.

DOI: 10.1103/PhysRevA.64.012718 PACS number(s): 34.50.Fa

I. INTRODUCTION

Inner-shell ionization of atoms induced by energetic heavy ions continues to play an inspiring role in the progress of various collision models. Even though this area of research is fairly old and a lot of improvements were incorporated in the theory, yet a lot of discrepancies are observed between the predictions of the models and the experimental data. It is customary to compare the measured ionization cross sections with the perturbed stationary state (PSS) approach including corrections due to the energy (E) loss of the projectile and its Coulomb (C) deflection in the field of the target nucleus, as well as, relativistic (R) effects (ECPSSR) [1]. This model explains very successfully the ionization data obtained using protons and alpha particles. A compilation of the proton- and alpha-particle induced *K*-shell ionization cross section data by Lapicki [2] illustrates the success of this model. The advantage of this model lies in the simple analytical expressions for calculating the cross sections. As compared to the ionization data using proton and alpha particles, similar data using heavy ions with $Z_1 \leqslant 16$ and targets with medium *Z* have shown large discrepancies between the measured cross sections and the predictions of this model [3–8]. Very recently Watson *et al.* [9] investigated in more detail the projectile *Z* dependence of Cu *K*-shell vacancy production at an energy of 10 MeV/u using a variety of projectiles from Ne to Bi. High-resolution x-ray spectra were taken to determine the appropriate fluorescence yields for converting the x-ray production cross sections to ionization cross sections. The cross sections show large deviations from the ECPSSR calculations for projectiles with $Z_1 \geqslant 18$.

In the case of high-*Z* elements the inner-shell electrons move at relativistic velocities. It therefore becomes essential to use the relativistic wave functions for the target electrons to compute the cross-section values. One expects significant differences in the calculated values depending on the wave functions used as the behavior of the relativistic and the nonrelativistic wave functions near the target nucleus is very different. The ECPSSR model takes nonrelativistic hydrogenic wave functions with approximate correction, in a phenomenological way, for the relativistic effects. It is therefore desirable to check the accuracy of these corrections for heavy-ion-induced data in high-*Z* elements. To the best of our knowledge very few such measurements exist. Burch *et al.* [10] investigated the *K*-shell ionization of Pb in collisions with 50–100-MeV-Cl ions. Awaya *et al.* [11] studied the *K*-shell ionization of several elements between Cr and Bi using 5 MeV/u N ions. Liatard *et al.* [12] performed *K*-shell ionization measurements on solid targets ranging in *Z* from 27 to 92 using 30 MeV/u Ne and Ar projectiles. Balster *et al.* [13] have measured *K* x-ray production cross sections for targets with atomic numbers ranging from 40 to 90 with beam energies varying between 4.5 and 13 MeV/u. Most of these measurements, which have been carried out at a fixed energy of the available cyclotrons, provide overall good agreement with the predictions of the ECPSSR theory but displaying small but systematic deviation from the theoretical projectile and target *Z* dependences. More recently, Kravchuk *et al.* [14] have studied the *K*-shell ionization of Pb induced by α, C, and O projectiles with energy 80 MeV/u and found very good agreement with the ECPSSR calculations. This is not surprising because this calculation is based on a perturbative model that works better at high energies. Apart from the ECPSSR model the calculations based on the semiclassical approximation (SCA) [15,16] also have been used to compute the ionization cross sections.

 ©2001 The American Physical Society

We report here *K*-shell ionization of Sb, Gd, Yb, Au, and Bi induced by F ions in the medium-energy range of 2.6–5.8 MeV/u where no such measurements exist. The measurements are aimed at further exploring relativistic effects that are known to affect the cross-section values.

II. THEORETICAL MODELS

The inner-shell electrons in a target like Au, or Bi move with relativistic velocities. Accordingly, one should use relativistic wave functions in the calculation of the relevant form factors that affect mainly the high-momentum tail of the wave function. Since the minimum momentum transfer to the electron in an ionization process increases with decreasing projectile velocity, this correction will be most important at small-impact parameters. The difference between relativistic and nonrelativistic treatment seems to be mainly attributable to the following effect.

The relativistic bound-state wave function varies as $r^{\gamma-1}\exp(-r)$ with $\gamma^2=1-(Z_2/137)^2$, and the nonrelativistic as $\exp(-r)$. Thus near the nucleus $(r\sim 0)$ the two behave differently. The relativistic wave function, because of the presence of the factor $r^{\gamma-1}$, has a week divergence at $r=0$ leading to an increased density of high-momentum components in the electronic momentum wave function. Therefore, the momentum transfer from the projectile to the target electron is more efficient with relativistic wave functions and larger cross sections are expected.

In the ECPSSR formalism, Brandt and Lapicki [1] have developed a relativistic correction to PWBA in a manner analogous to the way they accounted for the binding-energy effect. Instead of using the rest mass of the electron they used a local relativistic electron mass $m^R(r)$, through the virial theorem, for a relativistic electron in a central potential of the form Z_{2K}/r at a distance r from the target nucleus. The quantity $m^R(r)$is given by

$$m^R(r)=[1+(Z_{2K}/2rc^2)^2]^{1/2}+Z_{2K}/2rc(1+1.1y_K^2)^{1/2}+y_K \tag{1}$$

where $y_K=[0.4(Z_{2K}/c)^2]/\xi_K$ and $Z_{2K}=Z_2-0.3$. To get the relativistic cross section one has to transform the reduced velocity variable ξ_K to $\xi_K^R[=(m_K^R)^{1/2}\xi_K]$.

In the SCA approach used in Ref. [16], the projectile is assumed to move on a classical trajectory in the field of the screened target atom. The effects of the Coulomb deflection as well as the influence of the screening on the projectile trajectory are therefore fully accounted. The effect of the recoil of the target nucleus is also exactly taken into account. The binding energy of the target *K*-shell electron is chosen to be that for the united atom. This approximation is quite justified since the reduced velocities of the projectile, i.e., v_p/v_e vary between 0.12 and 0.3 (i.e., $\ll 1.0$) in the present collisions. The active electron is fully described by relativistic hydrogenic wave functions by solving the Dirac equation. In principle, one could also use relativistic Hartree-Fock-Slater wave functions to account for the screening by the outer electrons (see, e.g., Ref. [17]), but as has been shown in this reference for the energies and colliding systems in question, the use of relativistic hydrogenic (unscreened) wave functions is a very good approximation.

Amundsen *et al.* [18] have also presented an approximate formula for the ratio of the *K*-shell ionization cross sections with and without the inclusion of the relativistic effect in the target wave function.

III. EXPERIMENTAL DETAILS AND DATA ANALYSIS

The details of the experimental setup used in these measurements have been described earlier by Tribedi *et al.* [6]. Briefly, ion beams of F in the energy range 50–100 MeV were obtained from the BARC-TIFR Pelletron accelerator at Mumbai. The targets were mounted on a rotatable multiple-target-holder assembly in an electrically isolated chamber. Well-collimated beam was made to pass through the thin targets of Sb, Gd, Yb, Au, and Bi of thickness 34, 15, 40, 214, and 380 $\mu g/cm^2$, respectively, on 15-$\mu g/cm^2$-thick carbon backing. We have used some thick targets (Bi with 650 $\mu g/cm^2$ and Yb with 980 $\mu g/cm^2$) and found that there was no thickness- or charge-state dependence of the x-ray yields. This is expected as for these medium and high-*Z* targets the *K* electrons are so tightly bound that the probability of *K-K* or *K-L* charge transfer is negligible from the target to the highly charged F ions. The target x-rays were detected by an intrinsic Ge detector of 30-mm^2 diameter and 3-mm thickness mounted outside the vacuum chamber at an angle of 90° with respect to the beam direction. The detector had an energy resolution of 170 eV at 5.9 keV. Suitable absorbers of accurately known thickness were placed in front of the detector to reduce the intensities of the *L* and *M* x-rays from the target. The thickness of the targets was obtained during the measurements by counting the Rutherford-scattered particles in a Si-surface-barrier detector mounted at an angle of 135° with respect to the beam direction. The charge collected from the entire chamber was used for normalization.

Typical x-ray spectra obtained at a bombarding energy of 110 MeV are shown in Figs. 1(a–e) for each target used. The $K\alpha$ and $K\beta$ lines are well separated for all the targets. Except for Sb the $K\alpha_1$ and $K\alpha_2$ lines are also resolved. The intensities of the $K\alpha$ and the $K\beta$ group of lines were obtained separately using a standard peak-fitting program. These intensities were further corrected for efficiency of the detector as well as for the transmission of x rays through the absorber used. The measured value of the $K\alpha$-to-$K\beta$ intensity ratio agreed well with the theoretical values. No significant changes in the energy of the $K\alpha$ and $K\beta$ transitions (except for Sb) as well as their intensity ratios were observed as a function of the beam energy and therefore no change in the fluorescence yield (ω_K) values are expected. In the case of Sb a shift in the x-ray lines observed signifies the existence of multiple vacancies in the outer shells. However, considering the fact that ω_K is very large, the change in its value would be quite small.

Most of the cross-section data were obtained using the Rutherford-scattered particles from the target as normalization [see Eq. (2)]. However, in cases where the bombarding energy was close to or higher than the Coulomb barrier the

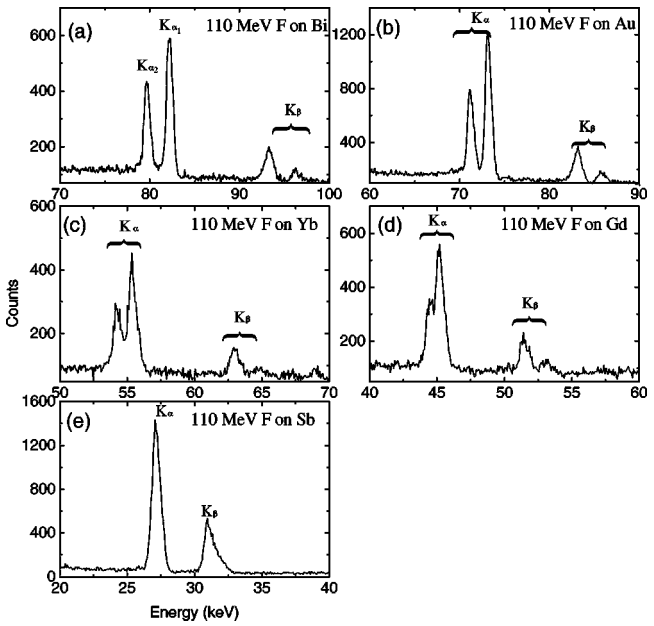

FIG. 1. The *K* x-ray spectra observed for various targets (as indicated) on bombardment with 5.8-MeV/u F ions.

charge collected on the chamber was used for normalization [see Eq. (3)]. Both sets of data, wherever possible, agreed within about 5–10 %. The overall experimental errors, arising from the uncertainties in the determination of the intrinsic efficiency of the detector, transmission through the absorber, solid angle of the detectors and the target thickness, were estimated to vary between 15–20 %.

The corrected values of the *K* x-ray peak intensity were used in deducing the x-ray production cross sections using the following expression:

$$\sigma_{KX} = \frac{4\pi N_x}{N_p \Delta\Omega_x \epsilon t}, \tag{2}$$

$$= \frac{4\pi N_x \Delta\Omega_p \sigma_R(\theta)}{N_t \Delta\Omega_x \epsilon}, \tag{3}$$

where N_x and N_t are the number of x rays and scattered particles detected, N_p the number of incident particles, t the target thickness, and ϵ the total efficiency of the x-ray detector including the transmission through the absorbers. The quantities $\Delta\Omega_x$ and $\Delta\Omega_p$ denote the solid angles subtended by the x-ray detector and the Si-surface-barrier detector, respectively, and $\sigma_R(\theta)$ the differential Rutherford scattering cross section. The x-ray production cross sections were obtained from the total area under the *K* x-ray peaks or by using only the $K\alpha$ intensity along with the theoretical $K\alpha/K\beta$ intensity ratio. The latter procedure was advantageous at the lowest bombarding energies where the cross sections were low. The ionization cross sections were obtained using the single-vacancy fluorescence yields tabulated by Krause [19]. These values, being high for the targets studied [ω_K varying between 0.87 (Sb) and 0.96 (Bi)], are not significantly affected by the multiple vacancies in the *L* and *M* shells, as discussed above. The ionization cross sections obtained along with other relevant quantities are shown in Table I and also in Figs. 2 to 4.

TABLE I. *K*-ionization cross sections σ_K^I (in barn) of Bi, Au, Yb, Gd, and Sb induced by F ions. The errors in the data points are about 15–20 %.

Energy (MeV)	Bi	Au	Yb	Gd	Sb
50	0.336	0.474	2.252	3.57	21.31
60	0.677	0.99	4.46		
65	0.67	1.22	5.31	9.17	46.40
70	1.12	1.69	6.14		
80	1.74	2.52	9.044		
83	1.769	2.52	9.07	14.51	94.43
90	2.63	4.09	12.463		
95	2.84	4.53	14.92	21.55	166.5
100	3.14	4.93	17.91		
110	4.20	6.17	21.23	33.77	235.1

IV. RESULTS AND DISCUSSIONS

A. Comparison with different models

The collision systems investigated are highly asymmetric with Z_1/Z_2 varying between 0.11 and 0.18. The velocity

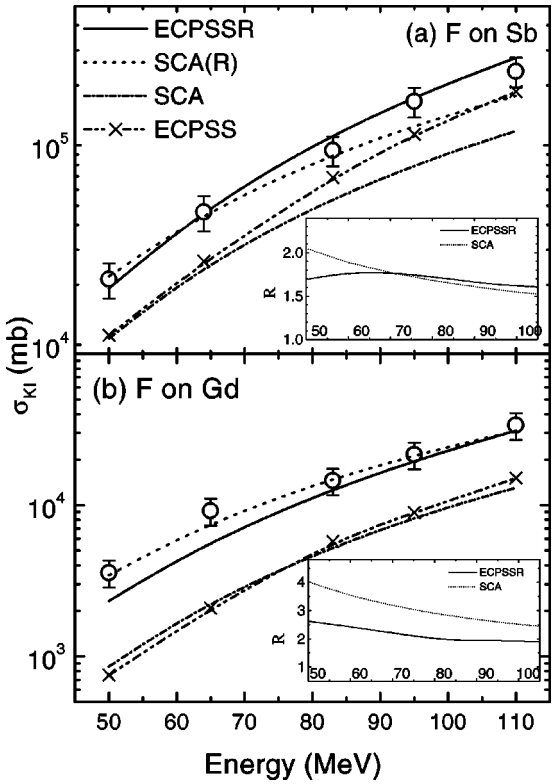

FIG. 2. Experimentally measured *K*-shell ionization cross sections for (a) Sb and (b) Gd plotted along with different theoretical predictions as a function of projectile energy. The symbols are explained in the figure. The ratio of the relativistic to nonrelativistic ionization cross sections obtained using various models are shown in the inset. The solid and dotted lines represent the ratios for the ECPSS and the SCA calculations.

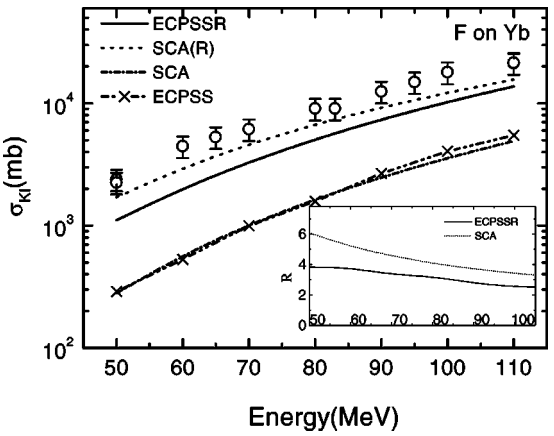

FIG. 3. Same as in Fig. 2 except for Yb target.

scaling parameter v_p/v_e spans a range of values between 0.12 and 0.29 indicating a slow or adiabatic collision. We have compared the present results with the predictions of different theoretical calculations in Figs. (2–4).

As mentioned earlier the relativistic effects will be most pronounced for high-Z targets. This can be ascertained from the calculated values of the cross sections with and without including the relativistic wave functions. According to both the models, this ratio R is found to be very sensitive to the energy of the incident projectiles as well as the target atomic number. As shown in insets in Figs. (2–4), in the SCA model the quantity R decreases as the energy of the incident particle increases and varies between 2 and 1.6 for Sb in the energy range investigated. In the extreme case of Bi it is found to vary between 17 and 9. This ratio is, however, smaller according to the ECPSSR prediction. Even though the extent of relativistic corrections in the calculations are somewhat different yet both the SCA and ECPSSR explain the experimental ionization data quite well. The SCA calculations show better agreement as compared to ECPSSR, especially for high-Z targets [see, for example, Figs. 2(b), 3, 4, and 5). The ECPSSR model on the other hand explains the data for Sb [Fig. 2(a)] extremely well with increasing deviation for heavier targets. It may be seen for high-Z targets like Gd, Yb, Au, and Bi that the nonrelativistic calculations, i.e., ECPSS and SCA agree with each other very well whereas the SCA(R) and ECPSSR differ from each other considerably. This fact could be linked to the magnitude of the relativistic effect as well as the phenomenological way in which these effects are introduced in the ECPSSR. If these effects are small, as in the case of Sb, the model explains the data very well. With increasing Z of the target the theory slightly underestimates the data. To illustrate this aspect we have plotted, in Fig 5, the ratios of the measured cross sections to the theoretical predictions for all the targets. The expected ratio, however, should be one that is shown by the horizontal dotted line. In case of Sb [Fig. 5(a)] the ratios of the measured cross sections to the ECPSSR predictions (open circles) remain very close to this ratio (dotted line) at all the energies. The ratios for the SCA calculations (squares) are very close to 1.0 except for the higher energies. From Figs. 5(b–e) it is obvious that in case of high-Z targets the ratio for the SCA calculations remain closer to the expected value than those for the ECPSSR. The large deviations in the case of Yb are difficult to understand particularly so when the

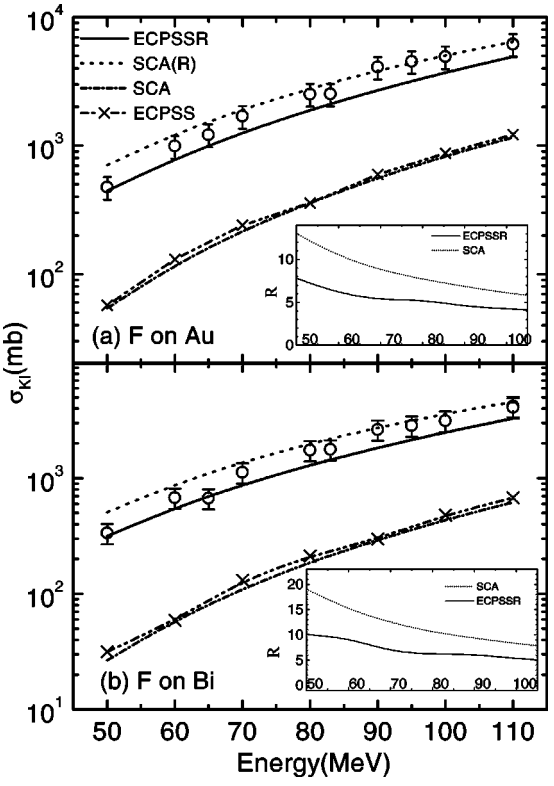

FIG. 4. Same as in Fig. 2 except for (a) Au and (b) Bi targets.

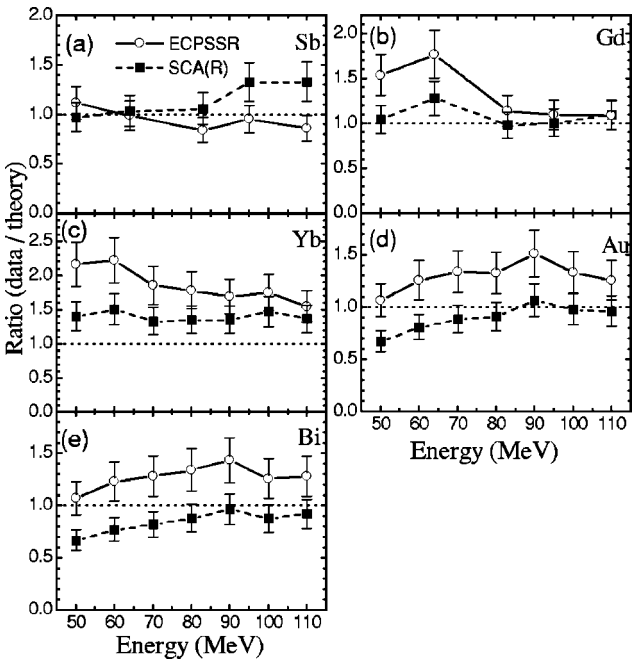

FIG. 5. Ratios of the measured data to the calculated cross sections using ECPSSR (circles joined by solid lines) and SCA(R) (squares joined by dashed lines). The different panels are for different targets.

data for Au and Bi are reasonably well understood by the ECPSSR theory. In these cases the relativistic effects are more pronounced than in Yb.

B. Universal scaling rule

According to the first-order perturbation theory properly scaled *K*-shell ionization (KI) cross sections are functions of scaled velocity only and do not depend on the actual target projectile combinations. It has been demonstrated in the past that if the scaled cross sections for KI are plotted as a function of the scaled velocity parameter then the different data sets fall on a universal PWBA curve [2]. Such scaling plots are very instructive. Not only do they indicate the global success of a theory but also are useful for various practical applications. Unfortunately a test of these scaling functions has been established for very-light projectiles and not too-heavy targets where relativistic effects are not so dominant [2]. Normally a plot of the ratio of the measured cross sections to the theory used has been discussed in literature where relativistic effects are strong. It has been shown by several workers that the measured KI cross sections, at least for light-ion projectiles on middle- or low-*Z* targets falls on the universal line when corrected according to the CPSS model [20,21] (also see Ref. [22] and references therein). But it remains to be seen whether such a universality still holds good after inclusion, in the CPSS, of the corrections due to the energy loss and relativistic effects, i.e., ECPSSR. The analytical formalism for such scaling procedure has not been worked out [1] before.

In the present investigation, since we are dealing mostly with heavy targets, it is educative to present the data in the form of scaled variables. We have plotted in Fig. 6(a) the reduced cross sections *without* taking the relativistic scaling into account in the ECPSS formalism. The scaled variables and the scaling procedure are defined in the literature [1,20,21]. In Fig. 6(b) we plot the reduced cross sections *with* taking the relativistic effect that are defined as [1],

$$\sigma_{red}^{ECPSSR}(\xi_K^R/\zeta_K)=\frac{\zeta_K\theta_K}{\sigma_{\circ K}}\frac{1}{C_K\left[\frac{2dq_{\circ K}\zeta_K}{z_K(1+z_K)}\right]}\frac{1}{f_K(z_K)}\sigma_{expt} \tag{4}$$

The quantity σ_{expt} denotes the measured cross section and the explanation of all other symbols can be found in Refs. [1,20,21]. As seen from Fig. 6(a) the scaled data for Yb, Au, and Bi for which the relativistic effects are most significant, fall almost on a common line and well separated from that of Sb and Gd for which such effects are not so significant. The data points also do not fall on the universal PWBA curve. After taking into account the relativistic effects [Fig. 6(b)] the data points now fall very close to a common line though the data points for Sb fall slightly below the rest. The universal PWBA function falls very close to the Sb and Gd data and underestimates those for high-*Z* targets as expected from the previous discussions. In order to investigate whether such universality really holds, one has to plot the scaled cross sections for different projectiles whereas the present discussions are limited for one projectile only.

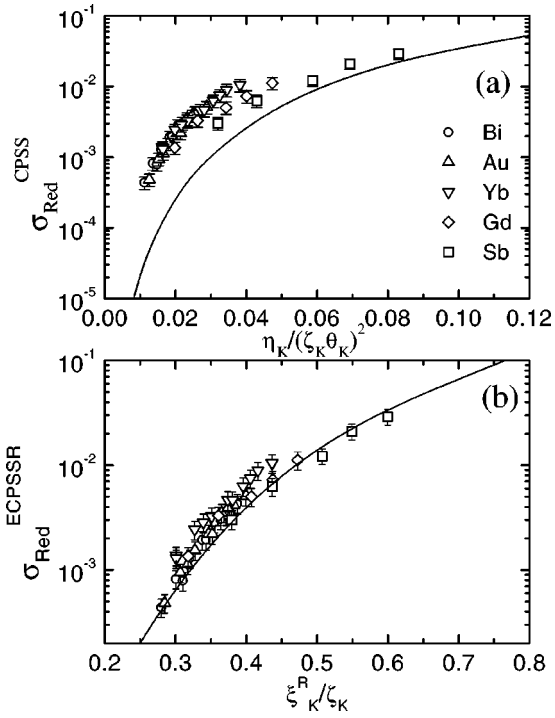

FIG. 6. Scaled cross sections for different targets in the (a) CPSS approach and (b) ECPSSR approach. The solid line is the universal PWBA function.

V. CONCLUSIONS

K-shell ionization cross sections are measured for selected medium- to high-*Z* targets ($Z\alpha=0.37$–0.61) by F-ion impact in the low- to intermediate-velocity range. The relativistic effects on the ionization cross sections are discussed. It is shown that the SCA calculations with the relativistic wave function predict an ionization cross section that is at least an order of magnitude higher compared to that given by nonrelativistic calculation for Bi target. This factor is reduced to about two for Sb. The contribution of the relativistic effect in the KI cross section is found to decrease with increase in the beam energy, as predicted by both the SCA and ECPSSR models. The results are in very good agreement with the SCA calculations including relativistic wave functions. The ECPSSR model although works quite well for medium-*Z* targets gives small deviations for the data for high-*Z* ($Z \geqslant 64$). In addition, it is shown that the ionization cross sections of high-*Z* (for which the relativistic effect is large) as well as low-*Z* targets (with less relativistic effect) can be scaled approximately according to ECPSSR scaling law so that all the data points follow a universal curve.

ACKNOWLEDGMENTS

The authors thank Umesh Kadhane and K. V. Thulasi Ram for their help during the measurements and the machine staff for the smooth operation of the machine.

[1] W. Brandt and G. Lapicki, Phys. Rev. A **23**, 1717 (1981), and references therein.
[2] G. Lapicki, J. Phys. Chem. Ref. Data **18**, 111 (1989).
[3] T.J. Gray, P. Richard, R.L. Kauffmann, T.C. Hollowag, R.K. Gardner, G.M. Light, and J. Guertin, Phys. Rev. A **13**, 1344 (1976).
[4] R.K. Gardner, Phys. Rev. A **19**, 1986 (1979).
[5] J.A. Tanis, S.M. Shafroth, W.W. Jacobs, T. McAbee, and G. Lapicki, Phys. Rev. A **31**, 750 (1985).
[6] L.C. Tribedi, K.G. Prasad, and P.N. Tandon, Phys. Rev. A **47**, 3739 (1993).
[7] L.C. Tribedi, K.G. Prasad, P.N. Tandon, Z. Chen, and C.D. Lin, Phys. Rev. A **49**, 1015 (1994).
[8] V. Horvat, G. Sampoll, K. Wohrer, M. Chabot, and R.L. Watson, Phys. Rev. A **46**, 2572 (1992).
[9] R.L. Watson, J.M. Blackadar, and V. Horvat, Phys. Rev. A **60**, 2959 (1999).
[10] D. Burch, W.B. Ingalls, M. Wieman, and R. Vandenbosch, Phys. Rev. A **10**, 1245 (1974).
[11] Y. Awaya, K. Izumo, T. Hamada, M. Okano, T. Takahashi, A. Hashizume, Y. Tendon, and T. Katou, Phys. Rev. A **13**, 992 (1976).
[12] E. Liatard, J.F. Bruandet, F. Glasser, T.U. Chan, G.J. Costa, C. Geradin, C. Heitz, M. Samri, and R. Seltz, Z. Phys. D: At., Mol. Clusters **2**, 223 (1986).
[13] G.J. Balster, W. van Huffelen, H.W. Wilschut, D. Chmielewska, and Z. Sujkowski, Z. Phys. D: At., Mol. Clusters **2**, 15 (1986).
[14] V.L. Kravchuk, A.M. Van den Berg, F.R.R. Fleurot, and H.W. Wilschut, KV9 Ann. Report No. P-30 (1999) (unpublished).
[15] J. Bang and J.M. Hansteen, Mat. Fys. Medd. K. Dan. Vidensk. Selsk. **31**, 13 (1959).
[16] D. Trautmann and F. Roseel, Nucl. Instrum. Methods Phys. Res. **214**, 21 (1983).
[17] Z. Halabuka, W. Perger, and D. Trautmann, Z. Phys. D: At., Mol. Clusters **29**, 151 (1994).
[18] P.A. Amundsen, L. Kocbach, and J.M. Hansteen, J. Phys. B **9**, L203 (1976).
[19] M.O. Krause, J. Phys. Chem. Ref. Data **8**, 307 (1979).
[20] G. Basbas, W. Brandt, and R. Laubert, Phys. Rev. A **7**, 983 (1973).
[21] G. Basbas, W. Brandt, and R. Laubert, Phys. Rev. A **17**, 1655 (1978).
[22] L.C. Tribedi and P.N. Tandon, Phys. Rev. A **45**, 7860 (1992).